Target Recognition of SAR Image Based on CN-GAN and CNN in Complex Environment

CONG MAO[1], LIZHEN HUANG[1], YONGSHENG XIAO[1], FENGSHOU HE[2], AND YUFAN LIU[1]
[1]School of Information Engineering, Nanchang Hangkong University, Nanchang 330063, China
[2]Leihua Electronic Technology Research Institute, Aviation Industries of China, Wuxi 214063, China

Corresponding author: Yongsheng Xiao (xysfly@nuaa.edu.cn)

ABSTRACT In recent years, with the rapid development of deep learning, the research of radar image automatic target recognition (ATR) has made great progress. However, because of the complex environments and special imaging principles, Synthetic Aperture Radar (SAR) image still have the problems of sample scarcity and strong speckle noise, which affects the target recognition performance. To solve the above problems, we proposed a target recognition method of SAR image based on Constrained Naive Generative Adversarial Networks (CN-GAN) and Convolutional Neural Network (CNN). Combining Least Squares Generative Adversarial Networks (LSGAN) and Image-to-Image Translation (Pix2Pix), CN-GAN can overcome these problems of low Signal-to-Clutter-Noise Ratio (SCNR), model instability and the excessive freedom degree of the output, which are produced by conventional naive GAN. Besides, we adopted a shallow network structure design in CNN, which can effectively improve the generalization ability of the model and avoid the problem of model overfitting. The experimental results in this paper demonstrate that CN-GAN has achieved the data generation and data enhancement, the SCNR of generated data is higher than the origin data set and data sets gained by other forms of GANs, the recognition performance based on the extended data set is better than the origin data set, and the recognition rate of data set enhanced by CN-GAN is higher than that of other common data enhancement methods.

INDEX TERMS Convolutional neural network, generative adversarial networks, synthetic aperture radar, target recognition.

I. INTRODUCTION

Compared to optical, infrared and other sensors, SAR is not influenced by the weather, light or other conditions, can achieve continuous observation in all weather, and has a certain surface penetration ability [1]. It has been widely used in civil and military fields [2]. At the same time, SAR technology has developed rapidly, with SAR image getting better quality and higher resolution, while the ATR development based on SAR image is relatively slower [3]. These difficulties of SAR ATR mainly focus on three aspects: (1) These complex environments including non-target clutter, occlusion, stacking, concealment, camouflage, electronic countermeasures, electromagnetic interference, etc., lead to the low SCNR problem; (2) The variation of the target itself and the difference of the same type target, for example, the variation of structure and connection, and the variants

caused by the target damage, account for sample scarcity; (3) The influence of imaging parameters includes elevation angle, frequency, imaging mode, polarization mode, number of sights, signal-to-noise ratio, resolution, etc., results in poor correlation among different targets, which makes the recognition method for one or several SAR targets cannot be quickly applied to other targets, that is, the effectiveness and adaptability of current recognition methods need to be improved [4], [5]. In recent years, the target recognition technology based on artificial intelligence represented by deep learning, has developed rapidly and achieved great success in the fields of text recognition, image recognition and speech recognition [6], [7]. It is the need of improving the recognition performance and development trend to applying artificial intelligence technology to SAR ATR. Nowadays, these deep learning models including Auto Encoder (AE), Deep Belief Networks (DBN), Convolution Neural Network (CNN) has been put into practice in terms of SAR ATR.

The associate editor coordinating the review of this manuscript and approving it for publication was Junjie Wu.

II. RELATED WORK

As a typical supervised feedforward deep learning model, CNN is superior to traditional machine learning methods in the matter of image target detection and recognition, and has also been well used in the field of SAR image target recognition. Ding *et al.* [8] referred to the VGGNet structure designed a CNN structure for SAR ATR, and used a smaller convolution kernel (3×3), in the MSTAR dataset, the classification accuracy of 10 categories containing variants was 93.16%. Chen *et al.* [9] proposed an all-convolutional networks (A-ConvNets), which used a larger convolution kernel (5×5, 6×6) and global average pooling instead of the full connection layer. Due to the reduction of model parameters, the classification accuracy of 10 classes of targets without variants can reach 99.13% under the condition of data enhancement.

But when CNN is used for SAR image recognition, there are still have the problems of sample scarcity and strong speckle noise, which easily exercise a negative influence on the recognition performance. Aiming at the sample scarcity problem, the usual method is to obtain enough training samples through data enhancement to improve the generalization ability of the model. Lin *et al.* [10] proposed a SAR image enhancement method based on target scattering center. Wagner [11] studied the impact of two data enhancement methods, affine transformation and elastic deformation, on the recognition accuracy of SAR images. Ding *et al.* [8] used translation, adding noise and Angle synthesis to obtain the enhanced training sample set, and the experimental results showed that these three data enhancement methods could greatly improve the classification accuracy of the model. Chen *et al.* [9] extracted sub-images with a resolution of 88×88 from images with a resolution of 128×128 by means of random cropping. Generating new samples by electromagnetic simulation is another method of data expansion in the field of SAR target recognition, such as RaySAR method. Auer [12] used ray tracing technology based on the three-dimensional model of the target to construct simulation samples. To solve the problem of SAR image with large speckle noise resulting in low SCNR, Chierchia *et al.* [13] added the logarithmic operation to transform the speckle noise model into additive noise model, so as to realize the denoising of SAR image. Wang *et al.* [14] and Wang *et al.* [15] use division to divide the noise image with the learned noise to obtain the denoised image. Wang *et al.* [15] added the combination of the denoising network and classification network to achieve the end-to-end denoising classification of SAR images, and achieved better classification results. Zhang *et al.* [16] used a combination of expanded convolution and skip connection with residual learning structure, and has achieved good results in the suppression of strong speckle noise.

Using GANs samples as extended data for classifier training has a good prospect, but due to GANs training difficulties, lack of stability, mode collapse and other problems, it is a challenging task to obtain extended samples that can effectively improve the performance of classifier through confrontation training. Guo *et al.* [17] proposed a generation method based on Conditional Generative Adversarial Nets (CGAN), which can solve the model collapse of CGAN through normalizing speckle noise. Gao *et al.* [18] presented a semi-supervised learning method based on standard Deep Convolutional Generative Adversarial Nets (DCGAN), which adopted two discriminators for joint training to generate higher-quality SAR images. Cui *et al.* [19] used Wasserstein Generative Adversarial Nets (WGAN) to generate expanded samples, and introduced a sample selection method of high-quality samples with specific azimuth angles from the generated samples. Merkle *et al.* [20] studied optical and SAR image matching method based on CGAN, and realized the generation from optical image block to SAR image block. Ley *et al.* [21] learned to transcode SAR images into optical images, and used CGAN to distinguish different land surfaces. In order to solve the problem of the missing azimuth of SAR images in the target domain, Ao *et al.* [22] proposed a Dialectical GAN for SAR image translation, which can transform a low-resolution SAR image with large ground coverage into a high-resolution SAR image. Liu *et al.* [23] adopted the principle of ray tracing to generate SAR simulation images under various azimuth angles. Bao *et al.* [24] introduced the Cycle-GAN algorithm, which transformed the image from the simulation domain to the real domain, and realized the data enhancement of the target domain image. Sagi *et al.* [25] putted forward the idea of rotatable hidden space. Through inputting two SAR images of different azimuth angles, the encoder-decoder structure is looked on as the hidden space feature representation of the input image, and a rotation transformation matrix is obtained by using the feature, and then SAR images of various azimuth angles is generated on the ground of the learned matrix. Song and Xu [26] designed a zero-sample learning model of target feature space based on deep generative neural network. The model includes three modules: constructor, generator and parser. The constructor converts the input sample label to the target feature space, the generator reconstructs the target image from the target azimuth information. Wang *et al.* [27] enhanced the quality of generated SAR image sample by improving the Wasserstein Autoencoder model structure and reconstruction error. According to Pan *et al.* [28] and Fengshou *et al.* [29], in contrast to other data expansion methods, the method based on GANs has greater advantages and application space from the aspect of image quality.

In view of the image scarcity, we proposed a new kind of GAN model, called CN-GAN. CN-GAN can generated new SAR images by inputing the original SAR image dataset. And aim at the low SCNR, we added different degrees of speckle noise to the original SAR dataset to simulate the interference problems brought by different environments, and then use CN-GAN to enhance the data of the image to improve the SCNR. So in this paper, the following contributions have been achieved:

(1) Generate the high quality SAR images through CN-GAN;

(2) Improve the SAR images SCNR through CN-GAN;

(3) Use a shallow network CNN architecture to test the recognition rate of the enhanced images by CN-GAN;

The rest of this paper is organized as follows. Section 3 gives an introduction of the principle of CN-GAN, the specific model structure design, parameter design, and CNN model structure design. In Section 4, the images generated experiments, augmentation experiments and recognition experiments are shown. And Section 5 is the conclusion of this paper.

III. METHODS

A. CN-GAN MODEL DESIGN

GAN is a new framework, which can generate the new samples through the adversarial process [30]. Two models can be trained at the same time, the generation model G is for capturing data distribution and the discriminant model D is for estimating the probability of samples from training data. The basic structure of GAN of SAR data generation is illustrated in Fig.1.
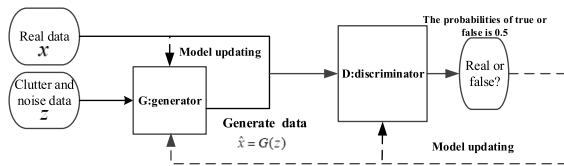

FIGURE 1. Basic structure of GAN of SAR data generation.

CN-GAN is based on GAN. The task of data generation is to generate data for a class of data with a small number of samples, and generate a great number of new samples that are similar to the real samples. In GANs, the relationship between G and D is expressed by the cost function, as the following equation.

$$
\begin{cases}
J^{(G)}(\theta^{(D)}, \theta^{(G)}) = \dfrac{1}{2}E_{x \sim P_{data}} + \dfrac{1}{2}E_{x \sim P_z}\log(1-(D(G(z)))\\
J^{(D)}(\theta^{(D)}, \theta^{(G)}) = -\dfrac{1}{2}E_{x \sim P_{data}} - \dfrac{1}{2}E_{x \sim P_z}\log(1-(D(G(z))))
\end{cases}
$$
$$(1)$$

where z is the clutter and noise data, and x is radar data.

We used a total function f represented $J^{(G)}$ and $J^{(D)}$

$$f(D, G) = E_{x \sim P_{data}(x)}[\log D(x)] + E_{x \sim P_z(x)}[\log(1-D(G(z)))] \tag{2}$$

where P_z (x) is the distribution function of the clutter and noise data, and P_{data} (x) is the radar signal data distribution function.

$$J^{(D)} = -\frac{1}{2}f(\theta^{(D)}, \theta^{(G)}) \tag{3}$$

$$J^{(G)} = \frac{1}{2}f(\theta^{(D)}, \theta^{(G)}) \tag{4}$$

In Game Theory, the decision-making combination of two sides of the game forms a Nash equilibrium point under which two sides cannot increase their own profits through their own

actions. For GANs, the Nash equilibrium point is to find the best $f(\theta^{(D)}, \theta^{(G)})$, so that the loss of G and the loss of D are both minimized, and then a minimax problem is formed, which is defined as

$$\arg \min_G \max_D f(D, G) \tag{5}$$

However, the vanishing gradient problem is prone to be happened for conventional naive GAN during the model learning. To solve this problem, we adopted the least-squares GAN [31] method, and formula (2) is transformed into an objective function in the sense of least squares as

$$
\begin{cases}
\min_G f(G) = E_{z \sim P_z(z)}[(D(G(z)) - 1)^2]\\
\min_D f(D) = E_{x \sim P_{data}(x)}[(D(x) - 1)^2]\\
\quad + E_{Z \sim P_z(z)}[(D(G(z)))^2]
\end{cases}
\tag{6}
$$

In addition, conventional naive GAN also exists the excessive output freedom problem, which often generates unreasonable samples that can deceive D. In terms of the problem, a regression function constraint item shown as formula (7), is added to the objective optimization function of G in order to minimize the mean square distance between the generated sample and the real signal. The regression function constraint item can reduce the degree of freedom of the output of G, so the improved GAN can resolve the problem of sample scarcity.

$$\xi(G) = E_{Z \sim P_z(z)}[(G(z) - x)^2] \tag{7}$$

And then, formula (6) is written as

$$
\begin{cases}
\min_G f(G) = E_{z \sim P_z(z)}[(D(G(z)) - 1)^2]\\
\quad + \lambda E_{z \sim P_z(z)}[(G(z) - x)^2]\\
\min_D f(D) = E_{x \sim P_{data}(x)}[(D(x) - 1)^2]\\
\quad + E_{z \sim P_z(z)}[(D(G(z)))^2]
\end{cases}
\tag{8}
$$

where λ represents the adjustment weight. The naive GAN with the above constraint term $\xi(G)$ is called Constrained Naive GAN (CN-GAN).

After the addition of $\xi(G)$, since the real data is visible to G, the training of G actually changes from unsupervised learning to supervised learning. In formula (8), the loss function of G is divided into two parts, one is the adversarial loss function, and the other is the sample distortion loss function. If the adversarial loss function is removed, the learning of G does not depend on D, and the learning of G is similar to the current mainstream deep learning based on a single deep neural network. Although the single deep neural network has a good nonlinear learning ability, when SCNR is low, the nonlinear learning ability will be reduced. From this point of view, CN-GAN guides the generator training through the discriminator, which can compensate for the design flaw of the loss function of the single-depth neural network and performance degradation due to low SCNR, and obtain better training results. Therefore, the radar data generation method based on CN-GAN is better than the previous method.
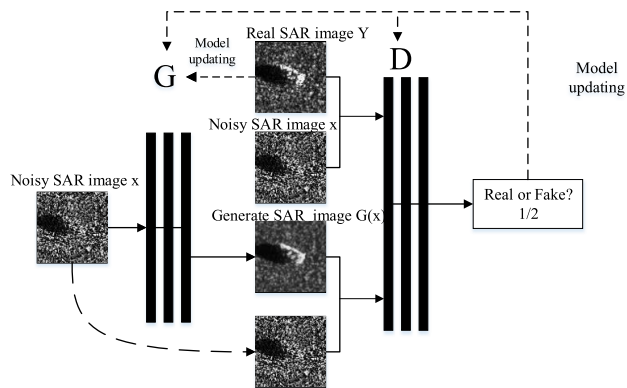
FIGURE 2. CN-GAN architecture diagram.

Furthermore, in order to directional generated the SAR images and improve the SCNR of SAR images, CN-GAN combined with the Image-to-Image generation (Pix2Pix) method [32],which changes from the random noise to speckle noise, so that the generated image quality can be improved. The overall architecture of the proposed CN-GAN is shown in Fig.2.

The network of CN-GAN in this paper follows the structure of DCGAN's network, which includes convolutional layer, Batch normalization and ReLU activation function. The network structure of CN-GAN generator and discriminator is shown in Fig.3.

Since the added regression function term represents the mean square distance between the generated sample and the real signal, it can be used to generate the contour and structure of the image, which corresponds to the low-frequency part of the image. While LSGAN is mainly used to generate these

details of the SAR image, which corresponds to the high frequency part of the image. During the training, the discriminator network adopts the idea of Patch-GAN and regards a part of the image as the receiving area of the discriminator. For the SAR image with the original size of 100×100, the pixels of 1×1, 16×16, 64×64 and the full image are carried out respectively. As a result, we found the image generated on the size of 64×64 has a higher restoration degree. The structure of U-Net is adopted to design the generator, which adds a jump connection into the codec structure, so that some useful repetitive information can be directly shared to the generator. The structure of U-Net is shown in Fig.4. Table 1 shows the setting parameters of CN-GAN.

TABLE 1. Parameters of the CN-GAN.

Parameters	Value
Learning rate	0.0002
Mini batch	64
Max Epochs	100
Activation function	ReLu

B. CNN MODEL DESIGN

We proposed a shallow network CNN architecture, as shown in Fig.5. CNN directly uses SAR images as the input, which can avoid the complex feature extraction process, and the features acquired by its local receptive domain have nothing to do with the translation, scaling and rotation of the image, so it can be directly used in SAR ATR. The features are extracted through CNN, and the output is sent to the Softmax classifier. The Softmax classifier is an extended version of the logistic regression two classifier, and is used to solve the multi-classification problem. Suppose the training set is
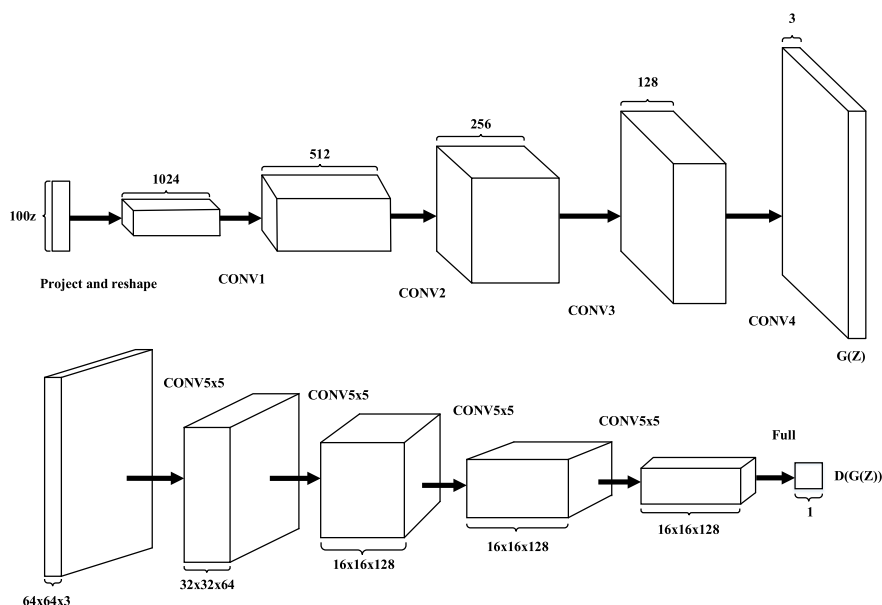

FIGURE 3. CN-GAN network structure diagram. The graph on the top shows the generator network structure, and the graph on the bottom shows the discriminator network structure.
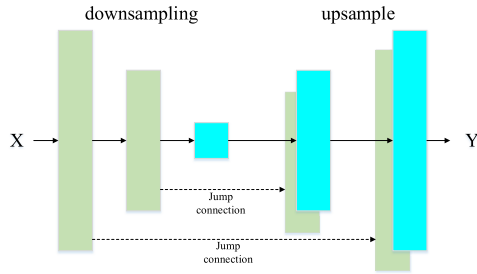
FIGURE 4. U-Net network structure.

(x_1,y_1),(x_2,y_2),...,(x_m,y_m) and $y_m \in \{0, k\}$, where m is the number of samples. The hypothetical function is shown in formula (9).

$$h_\theta(x^{(i)}) = [P(y^{(i)}) = 1|x^{(i)}; \theta) \cdots P(y^{(i)}) = k|x^{(i)}; \theta)]^T$$
$$= \frac{1}{\sum_{j=1}^k e^{\theta_j^T}} [e^{\theta_1^T x^{(i)}} e^{\theta_2^T x^{(i)}} \cdots e^{\theta_k^T x^{(i)}}]^T \quad (9)$$

where T is the network moment, θ is the parameter of the Softmax classifier, k is the number of categories of the classification results, and the hypothesis function represents the probability of each category, which is showed as

$$\theta = [\theta_1^T \theta_2^T \cdots \theta_k^T]^T \quad (10)$$

According to the maximum likelihood estimation, the loss function of the classifier is

$$J(\theta) = -\frac{1}{m}[\sum_{i=1}^m \sum_{j=1}^k o\{y^{(i)} = j\} \log \frac{e^{\theta_j^T x^{(i)}}}{\sum_{l=1}^k e^{\theta_l^T x^{(i)}}}] \quad (11)$$

where o(true)=1 and o(false)=0. The gradient descent method is utilized for the training, updating parameters, and minimizing the loss function of the classifier. Table 2 shows the specific parameters of CNN.

TABLE 2. Parameters of the CNN.

Parameters	Value
Learning rate	0.0005
Mini batch	16
Max Epochs	300
Activation function	ReLu

IV. EXPERIMENTAL RESULTS AND DISCUSSION

The dataset used in this paper is the MSTAR dataset. The acquisition conditions for MSTAR dataset are divided into two categories, Standard Operating Condition (SOC) and Extended Operating Condition (EOC). The dataset of SOC is adopted, which include 10 types of ground targets, as shown in Table 3. The training set was collected at 17° from the imaging side perspective, and the testing set was collected at 15° from the side perspective.

TABLE 3. Data type under SOC condition of MSTAR dataset.

Type	2S1	BRDM2	BTR60	D7	SN13
Train (17°)	299	298	256	299	232
Test (15°)	274	274	195	274	196
Type	SN9563	SNC71	T62	ZIL131	ZSU234
Train (17°)	233	233	299	299	299
Test (15°)	195	196	273	274	274

A. SAR IMAGE GENERATION EXPERIMENTS

For the preprocessing of training images, the training images are scaled to the range of $[-1, 1]$ by the activation function. The model is trained with mini-batch stochastic gradient descent. During the training CN-GAN model, we put all the 10 types military targets into the training model to train, the resolution of the input SAR image is 100×100, and we adapted the Adam optimizer. The model learning rate is set
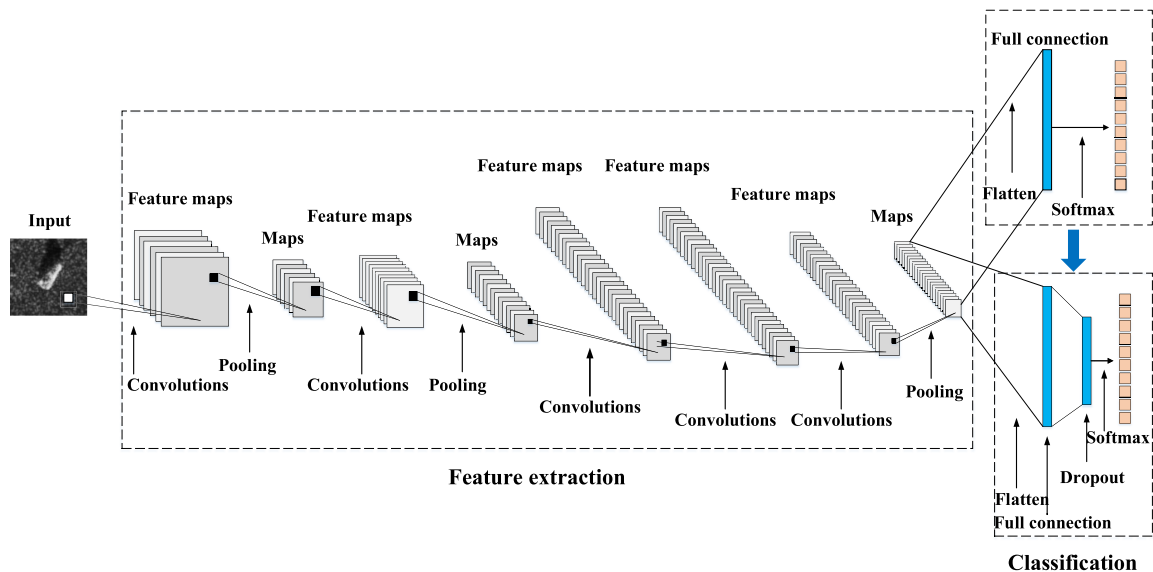

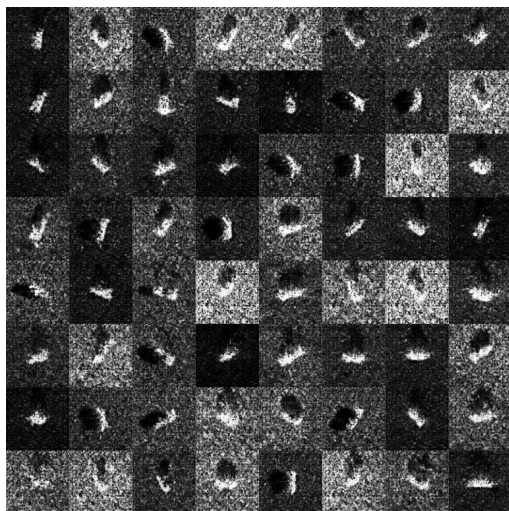**FIGURE 5.** SAR ATR method based on the shallow network structure CNN.

FIGURE 6. The result of CN-GAN with epoch=50.

Method	Recognition rate
CNN(L=1)	83.56%
CN-GAN+CNN(L=1)	90.14%
CNN(L=2)	86.47%
CN-GAN+CNN(L=2)	93.36%
CNN(L=3)	86.63%
CN-GAN+CNN(L=3)	95.17%
CNN(L=4)	90.16%
CN-GAN+CNN(L=4)	96.82%
CNN(L=5)	93.18%
CN-GAN+CNN(L=5)	98.75%
CNN(original SAR image)	99.17%
CN-GAN+CNN(original SAR image)	99.52%

to 0.0002, and the batch is set to 64. Some generated samples by CN-GAN is shown in Fig.6.

Since SAR images are easily affected by complex environments, in order to prove the universality of CN-GAN to generate samples to solve the problem of less samples in SAR images, we added different levels Rayleigh noise (The noise level L=1,2,3,4,5) into the original data to simulate different levels of interference problems, and then performed data generation and recognition rate tests on the data containing different levels of noise.

After 100 epoch iterations, the CN-GAN training model has been build. then we inputted 10 types of military training data into the trained CN-GAN model successively to obtain 10 types of generated samples. Then, we added the 10 types generated samples into the 10 types original data, as the expansion of the training data.

Finally, we used the CNN model to train the expansion of the training data, and test it with the test set to get the recognition rate. The recognition rate compared with SAR image without data generation was showed in Table 4.

It can be seen from Table 4, the recognition rate of the original dataset measured by using CNN in this paper is 99.17%, and the recognition rate is 99.52% after adding the generated data, the recognition rate is improved.

By comparing the recognition rates of SAR images under different noise levels with the recognition rates after addition the generated data, it can be seen that the recognition rate is

only 83.56% when the noise level is 5, while the recognition rate after the addition of generated data is 90.14%, which is a relative increase of nearly 7%. As can be seen from other results in the table, under the influence of different levels of noise, the recognition rate can be improved to a certain extent by adding generated data. Therefore, it can be proved that the generated data can not only improve the recognition rate of the original data, but also greatly improve the recognition rate under the condition of noise interference.

In consequence, using CN-GAN to generate new samples can solve the problem of fewer samples in SAR images to a certain extent.

B. SAR IMAGE ENRICHMENT EXPERIMENTS

To prove the CN-GAN model can improve the SAR images SCNR, these speckle noises with the mean value of 0 and the variance of 0, 0.5, 1.0, 1.5, 2.0, 2.5, 3.0, 3.5, 4.0, 4.5 and 5.0 are added respectively to the original MSTAR dataset. The SAR images with different degree speckle noise example showed in Fig.7.

Then the data with different noises are inputted to the CN-GAN generator in turn. The SAR image data containing noise is paired with the image generated by the generator, and the SAR image data containing noise is paired with the original SAR image data. The two sets of data are used together as the input of the discriminator to discriminate. The paired image formed by the former is judged to be false by the discriminator, while the paired image formed by the latter is judged to be true. After 100 epoch iterations, the loss function of the discriminator reach stability, the image quality generated is close to the original image, and the noise is suppressed. The SAR image data containing the speckle noise as the
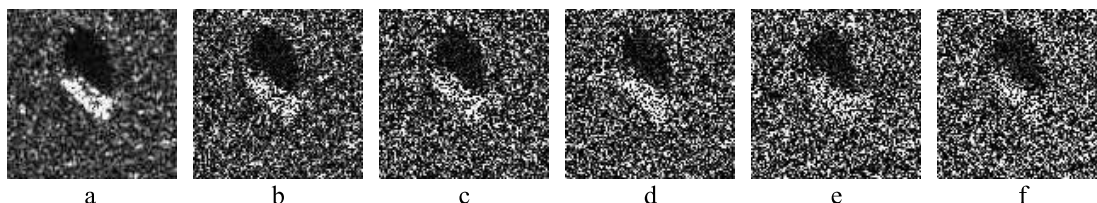

FIGURE 7. SAR images with different speckle noise. The variance of a=0, b=1, c=2, d=3, e=4, f=5.
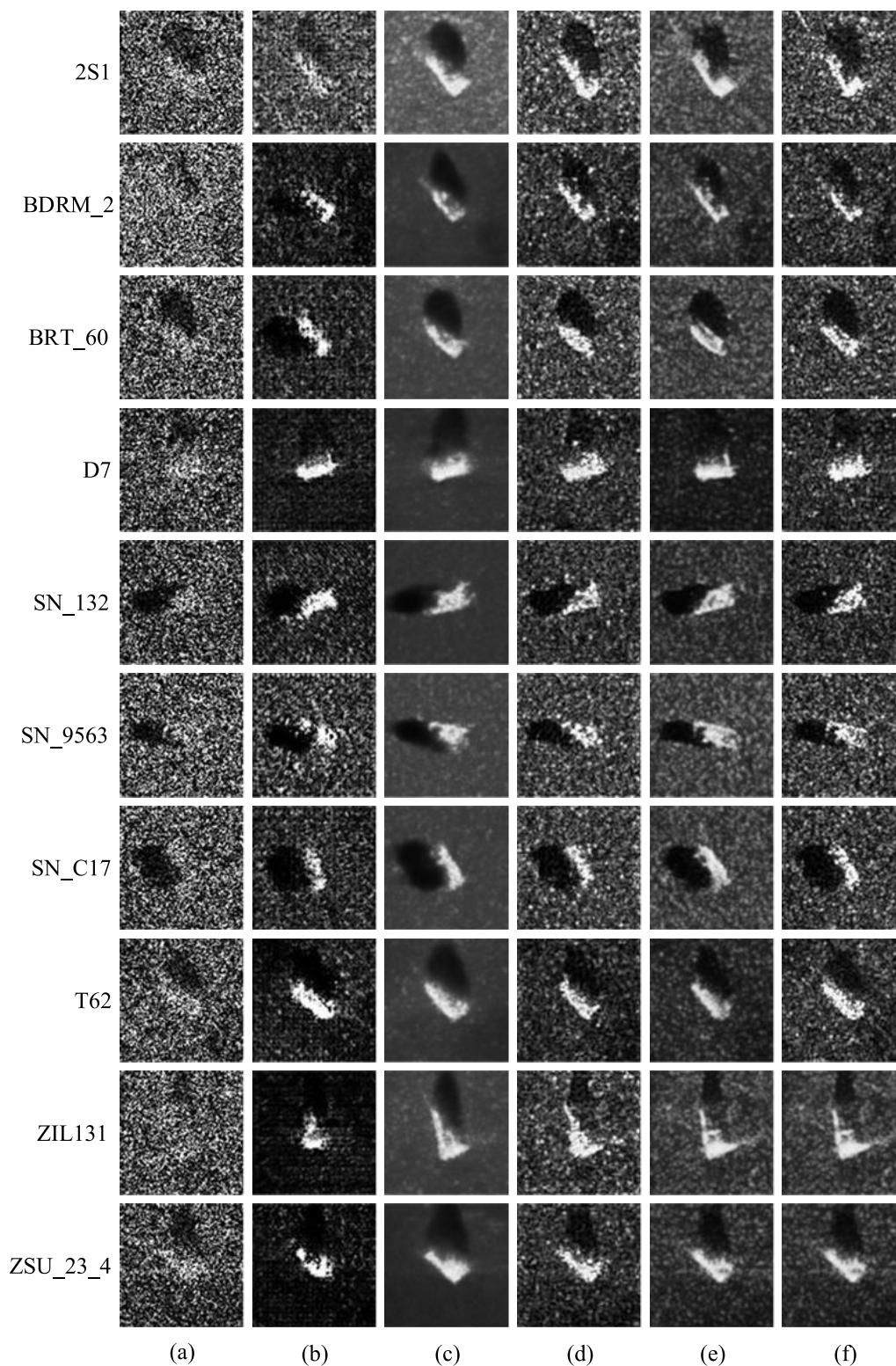
FIGURE 8. Ten categories of SAR images. (a) Noisy image, (b) DCGAN generated image, (c) LSGAN generated image, (d) CGAN+L1 loss generated image, (e) CN-GAN generated image, (f) original image.

train dataset is unified to be input to the Conditional GAN with L1 loss (CGAN + L1) network, LSGAN network, and DCGAN network. After the training, there are four models.

And then ten kinds of SAR image respectively as test data are input into the trained model in turn, and ten types of output SAR images are shown in Fig.8.

1) QUALITY EVALUATION

In order to objectively evaluate the quality of SAR images generated by different GANs, we measured the peak signal-to-noise ratio (PSNR), structural similarity (SSIM) and edge retention coefficient (EPI) of SAR images generated by four kinds of GANs, the original SAR image and the SAR image with noise. The measured data are shown in Table 5.

TABLE 5. The quality evaluation results of SAR images generated by different GAN.

SAR image type	PSNR	SSIM	EPI
Noise image	8.75	0.142	0.5782
DCGAN generates image	10.36	0.585	0.7424
LSGAN generates image	18.24	0.547	0.7633
CGAN+L1 loss generates image	14.52	0.724	0.8241
CN-GAN generates image	17.85	0.782	0.8252
Original image	16.47	0.752	0.7913

In this table, we can see that the PSNR of the data generated by CN-GAN is 17.85, is higher than original image (16.47), CGAN+L1 loss generated image (14.52), DCGAN generated image (10.36), and noise image (8.75). SSIM and EPI are higher than all other GANs' generated image and original image.

TABLE 6. The quality evaluation results of SAR images generated by different GAN.

SAR image type	Recognition rate
Noise image	88.66%
DCGAN generates image	90.03%
LSGAN generates image	93.62%
CGAN+L1 loss generates image	95.06%
CN-GAN generates image	99.42%

2) RECOGNITION PERFORMANCE

We adopted the CNN proposed in this paper to test the recognition rate. We used the 10 types augmentation data as the original training data, and inputted into CNN as a training set for training, then we used the test set from the original data to detect the recognition rate. Table 6 shows the recognition rate of different GANs generated SAR images. Fig.9 is the recognition rate curve of images generated by different GANs on the training set with the same multiplier noise input. Fig.10 is the line graph of the classification accuracy of images generated under different GANs with different degrees of speckle noise.

From these table and figures, it can be seen that the recognition rate results based on the generated data of fours forms of GANs are higher than the original noise data which are not done the process of data generation. Therefore, data generation is very necessary for the target recognition. And the recognition rate based on the data generated by other generation networks is lower than the result of CN-GAN. When the variance of coherent speckle noise is 0.5, the data set generated by CGAN+L1, DCGAN and LSGAN is respectively 95.06%, 90.03%, and 93.62%, they are inferior to the data set generated by CN-GAN (99.42%). It shows that the
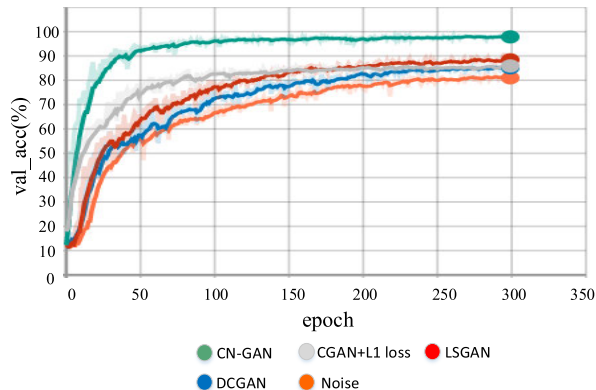

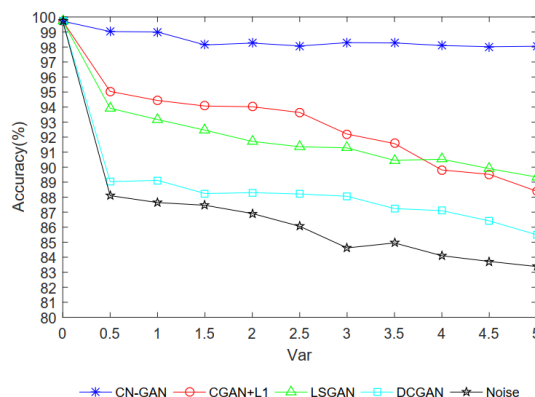**FIGURE 9.** The recognition rate graph.

FIGURE 10. The recognition rat of images generated with different degrees of multiplicative noise.

quality of the generated data of CN-GAN is better than the quality of the generated data by other forms of GANs. From the Figure 10 we can see that with the increase of speckle noise, the recognition rate will decrease under the influence of noise. However, the data enhanced by CN-GAN can still achieve a good recognition rate, which remains above 98%. but the recognition rate of the data obtained by other GANS decreases rapidly with the increase of noise, which indicates that the use of CN-GAN to enhance SAR images can reduce the influence brought by noise.

In order to prove the effectiveness of the data enhancement method, we introduce the results measured on the original MSTAR dataset by VGGNet in Reference [8] and the results measured on the original MSTAR dataset by A-ConvNets in Reference [9], and use CNN mentioned in this paper to detect the recognition rate on the original data set. Then, we replaced the training set of the original MSTAR data set with the data set denoised by CN-GAN, and used the above three recognition rate methods to test the recognition rate of the denoised SAR image. The comparison results are shown in Table 7.

By comparing the recognition rate of SAR image denoised by CN-GAN with the recognition rates without denoised, it can be found that the recognition rate is improved after

TABLE 7. The recognition rate measured by the three recognition methods under the condition of denoising and undenoising.

Methods	Recognition rate
VGGNet [8] (undeniosed)	93.16%
CN-GAN+VGGNet(denoised)	98.68%
A-ConvNets [9] (undeniosed)	99.13%
CN-GAN+A-ConvNets(denoised)	99.37%
CNN(undeniosed)	99.17%
CN-GAN+CNN (denoised)	99.42%

denoising compared with the recognition rate measured by the undenoised data set. It can prove that CN-GAN, as a new data enhancement method, enhances the SCNR of SAR image to enhance the data, so as to achieve a better effect in the target recognition of SAR image.

V. CONCLUSION

LSGAN has the advantage of model stability and high quality of image generation compared to conventional naive GAN, while Pix2Pix can get over the shortcoming of low SCNR caused by conventional naive GAN through inputting speckle noise images. We proposed a SAR image generation method based on CN-GAN, which combines LSGAN and Pix2Pix. In terms of LSGAN, a constraint term of regression function is added to the generator's loss function to reduce the mean square distance between the generated sample and the real sample. With regard to Pix2Pix, random noise is replaced by the noise images inputted to LSGAN. On the basic of the conventional CNN model, a shallow network structure is designed to avoid the problem of high model complexity and overfitting caused by the excessive deep network structure, so as to improve the recognition performance. MSTAR data set was applied to the generative model training and target recognition experiment. These results proved that CN-GAN can well solve the problems of SAR images with few samples and strong speckle noise, that is, the method solved these problems of excessive output freedom caused by conventional naive GAN, high training complexity of constrained GAN and model instability under low SCNR. In subsequent research, the effective combination of CNN and attention mechanism, the optimization of the network structure and parameter adjustment, will be further researched, so that CNN can even better obtain effective information about the recognition.

REFERENCES

[1] G. Franceschetti and R. Lanari, *Synthetic Aperture Radar Processing*. Boca Raton, FL, USA: CRC Press, 1999.

[2] C. Oliver and S. Quegan, *Understanding Synthetic Aperture Radar Images*. Rijeka, Croatia: SciTech, 2004.

[3] D. J. Crisp, "The state of the art in ship detection in synthetic aperture radar imagery," Aust. Gov., Dept. Defence, Edinburgh, SA, Australia, Tech. Rep. DSTO-RR-0272, 2004.

[4] M. Cetin, I. Stojanovic, O. Onhon, K. Varshney, S. Samadi, W. C. Karl, and A. S. Willsky, "Sparsity-driven synthetic aperture radar imaging: Reconstruction, autofocusing, moving targets, and compressed sensing," *IEEE Signal Process. Mag.*, vol. 31, no. 4, pp. 27–40, Jul. 2014.

[5] F. Argenti, A. Lapini, T. Bianchi, and L. Alparone, "A tutorial on speckle reduction in synthetic aperture radar images," *IEEE Geosci. Remote Sens. Mag.*, vol. 1, no. 3, pp. 6–35, Sep. 2013.

[6] Y. LeCun, Y. Bengio, and G. Hinton, "Deep learning," *Nature*, vol. 521, no. 7553, pp. 436–444, May 2015.

[7] G. Hinton, L. Deng, D. Yu, G. Dahl, A.-R. Mohamed, N. Jaitly, A. Senior, V. Vanhoucke, P. Nguyen, T. Sainath, and B. Kingsbury, "Deep neural networks for acoustic modeling in speech recognition: The shared views of four research groups," *IEEE Signal Process. Mag.*, vol. 29, no. 6, pp. 82–97, Nov. 2012.

[8] J. Ding, B. Chen, H. Liu, and M. Huang, "Convolutional neural network with data augmentation for SAR target recognition," *IEEE Geosci. Remote Sens. Lett.*, vol. 13, no. 3, pp. 364–368, Mar. 2016.

[9] S. Chen, H. Wang, F. Xu, and Y.-Q. Jin, "Target classification using the deep convolutional networks for SAR images," *IEEE Trans. Geosci. Remote Sens.*, vol. 54, no. 8, pp. 4806–4817, Aug. 2016.

[10] Z. Lin, K. Ji, M. Kang, X. Leng, and H. Zou, "Deep convolutional highway unit network for SAR target classification with limited labeled training data," *IEEE Geosci. Remote Sens. Lett.*, vol. 14, no. 7, pp. 1091–1095, Jul. 2017.

[11] S. A. Wagner, "SAR ATR by a combination of convolutional neural network and support vector machines," *IEEE Trans. Aerosp. Electron. Syst.*, vol. 52, no. 6, pp. 2861–2872, Dec. 2016.

[12] S. J. Auer, "3D synthetic aperture radar simulation for interpreting complex urban reflection scenarios," Ph.D. dissertation, Deutsche Geodätische Kommission, Reihe C, Verlag der Bayerischen Akademie der Wissenschaften, Munich, Germany, 2011, no. 660, p. 126. [Online]. Available: http://dgk.badw.de/fileadmin/docs/c-660.pdf

[13] G. Chierchia, D. Cozzolino, G. Poggi, and L. Verdoliva, "SAR image despeckling through convolutional neural networks," in *Proc. IEEE Int. Geosci. Remote Sens. Symp. (IGARSS)*, Jul. 2017, pp. 5438–5441.

[14] P. Wang, H. Zhang, and V. M. Patel, "SAR image despeckling using a convolutional neural network," *IEEE Signal Process. Lett.*, vol. 24, no. 12, pp. 1763–1767, Dec. 2017.

[15] J. Wang, T. Zheng, P. Lei, and X. Bai, "Ground target classification in noisy SAR images using convolutional neural networks," *IEEE J. Sel. Topics Appl. Earth Observ. Remote Sens.*, vol. 11, no. 11, pp. 4180–4192, Nov. 2018.

[16] Q. Zhang, Q. Yuan, J. Li, Z. Yang, and X. Ma, "Learning a dilated residual network for SAR image despeckling," *Remote Sens.*, vol. 10, no. 2, p. 196, Jan. 2018.

[17] J. Guo, B. Lei, C. Ding, and Y. Zhang, "Synthetic aperture radar image synthesis by using generative adversarial nets," *IEEE Geosci. Remote Sens. Lett.*, vol. 14, no. 7, pp. 1111–1115, Jul. 2017.

[18] F. Gao, Y. Yang, J. Wang, J. Sun, E. Yang, and H. Zhou, "A deep convolutional generative adversarial networks (DCGANs)-based semi-supervised method for object recognition in synthetic aperture radar (SAR) images," *Remote Sens.*, vol. 10, no. 6, p. 846, May 2018.

[19] Z. Cui, M. Zhang, Z. Cao, and C. Cao, "Image data augmentation for SAR sensor via generative adversarial nets," *IEEE Access*, vol. 7, pp. 42255–42268, 2019.

[20] N. Merkle, S. Auer, R. Muller, and P. Reinartz, "Exploring the potential of conditional adversarial networks for optical and SAR image matching," *IEEE J. Sel. Topics Appl. Earth Observ. Remote Sens.*, vol. 11, no. 6, pp. 1811–1820, Jun. 2018.

[21] A. Ley, O. Dhondt, S. Valade, R. Haensch, and O. Hellwich, "Exploiting GAN-based SAR to optical image transcoding for improved classification via deep learning," in *Proc. 12th Eur. Conf. Synth. Aperture Radar*. Aachen, Germany: VDE, 2018, pp. 1–6.

[22] D. Ao, C. O. Dumitru, G. Schwarz, and M. Datcu, "Dialectical GAN for SAR image translation: From Sentinel-1 to TerraSAR-X," *Remote Sens.*, vol. 10, no. 10, p. 1597, Oct. 2018.

[23] L. Liu, Z. Pan, X. Qiu, and L. Peng, "SAR target classification with CycleGAN transferred simulated samples," in *Proc. IEEE Int. Geosci. Remote Sens. Symp. (IGARSS)*, Jul. 2018, pp. 4411–4414.

[24] F. Bao, M. Neumann, and N. T. Vu, "Cyclegan-based emotion style transfer as data augmentation for speech emotion recognition," in *Proc. Interspeech*, 2019, pp. 2828–2832.

[25] K. Sagi, T. Toizumi, and Y. Senda, "Rollable latent space for azimuth invariant SAR target recognition," in *Proc. IEEE Int. Geosci. Remote Sens. Symp. (IGARSS)*, Jul. 2018, pp. 21–24.

[26] Q. Song and F. Xu, "Zero-shot learning of SAR target feature space with deep generative neural networks," *IEEE Geosci. Remote Sens. Lett.*, vol. 14, no. 12, pp. 2245–2249, Dec. 2017.

[27] K. Wang, G. Zhang, Y. Leng, and H. Leung, "Synthetic aperture radar image generation with deep generative models," *IEEE Geosci. Remote Sens. Lett.*, vol. 16, no. 6, pp. 912–916, Jun. 2019.

[28] B. Zhang, Q. An, and Z. Pan, "Progress of deep learning-based target recognition in radar images," *Scientia Sinica Informationis*, vol. 49, no. 12, pp. 1626–1639, Dec. 2019.

[29] H. Fengshou, H. You, L. Zhunga, and X. Cong'an, "Research and development on applications of convolutional neural networks of radar automatic target recognition," *J. Electron. Inf.*, vol. 42, no. 1, pp. 119–131, 2020.
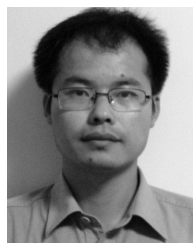
[30] I. Goodfellow, J. Pouget-Abadie, M. Mirza, B. Xu, D. Warde-Farley, S. Ozair, A. Courville, and Y. Bengio, "Generative adversarial nets," in *Proc. Adv. Neural Inf. Process. Syst.*, 2014, pp. 2672–2680.

[31] X. Mao, Q. Li, H. Xie, R. Y. K. Lau, Z. Wang, and S. P. Smolley, "Least squares generative adversarial networks," in *Proc. IEEE Int. Conf. Comput. Vis. (ICCV)*, Oct. 2017, pp. 2794–2802.

[32] P. Isola, J.-Y. Zhu, T. Zhou, and A. A. Efros, "Image-to-Image translation with conditional adversarial networks," in *Proc. IEEE Conf. Comput. Vis. Pattern Recognit. (CVPR)*, Jul. 2017, pp. 1125–1134.
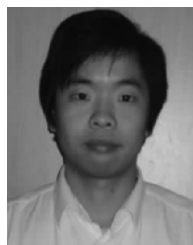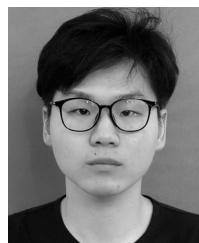
YONGSHENG XIAO was born in 1980. He received the Ph.D. degree from the Nanjing University of Aeronautics and Astronautics (NUAA), in 2014.

He is an Associate Professor with Nanchang Hangkong University. His research interests include radio frequency stealth (RFS) radar signal design, image processing, and pattern recognition.

CONG MAO was born in Pingxiang, Jiangxi, China, in 1997. He received the B.S. degree in electronic information engineering from Nanchang Hangkong University, Nanchang, Jiangxi, in 2019, where he is currently pursuing the master's degree.

His main research interests include SAR image target recognition and deep learning.

FENGSHOU HE was born in 1979. He received the master's degree from Xi'an Jiaotong University, in 2006. He is currently pursuing the Ph.D. degree with Northwestern Polytechnical University.

From 2008 to 2012, he was an Engineer with the AVIC Leihua Electronic Technology Institute, Wuxi, China, where he became a Senior Engineer, in 2012. He is currently the Director of the Science and Technology Development Department. His research interests include target recognition, information fusion, and intelligence radar.

LIZHEN HUANG was born in 1982. She received the Ph.D. degree from the Nanjing University of Aeronautics and Astronautics (NUAA), in 2016.

She is currently a Lecturer with Nanchang Hangkong University. Her research interests include image processing and pattern recognition and field-optic communication.

YUFAN LIU was born in Ganzhou, Jiangxi, China, in 2001. He is currently pursuing the bachelor's degree with Nanchang Hangkong University.

His research interests include deep learning and generative adversarial networks.

• • •